Anti-tumor Effects of Toxins Targeted to the Prostate Specific Membrane Antigen

Giulio Fracasso,[1] Giuseppe Bellisola,[1,2] Sara Cingarlini,[1] Deborah Castelletti,[1] Tommaso Prayer-Galetti,[3] Francesco Pagano,[3] Giuseppe Tridente,[1] and Marco Colombatti[1]*

[1]*Section of Immunology, Department of Pathology, University of Verona, Verona, Italy*
[2]*Azienda Ospedaliera di Verona, Verona, Italy*
[3]*Section of Urology, Department of Oncological and Surgical Sciences, University of Padua, Padua, Italy*

BACKGROUND. There is presently no effective therapy for relapsing, metastatic, androgen-independent prostate cancer. Immunotherapy with monoclonal antibody–vehicled toxins (Immunotoxins, ITs) may be a promising novel treatment option for the management of prostate cancer in these cases.
METHODS. Three anti–prostate specific membrane antigen (anti-PSMA) monoclonals (J591, PEQ226.5, and PM2P079.1) were cross-linked to ricin A-chain (RTA; native or recombinant), and their cytotoxic effects were investigated in monolayer and three-dimensional (3-D) cell cultures of prostate carcinoma cells (LNCaP).
RESULTS. The various Immunotoxins showed effects in the nanomolar range (IC_{50s} of 1.6–99 ng/ml) against PSMA+ cells (IC_{50} being the concentration inhibiting 50% cell proliferation or protein synthesis). $PSMA^-$ cell lines were 62- to 277-fold less sensitive to anti-PSMA ITs, evidencing an appreciable therapeutic window. Treatment with J591-smpt-nRTA (0.35–31.7ng/ml) resulted in complete eradication of 3-D tumor micromasses or in 1.46- to 0.35-log reduction of target cells number, depending on the dose.
CONCLUSION. Anti-PSMA ITs appear to be promising for use in the eradication of small prostate tumor cell aggregates present in tissues and in the bone marrow. *Prostate 53: 9–23, 2002.* © 2002 Wiley-Liss, Inc.

KEY WORDS: **prostate carcinoma; Immunotoxins; ricin; spheroids; immunotherapy; prostate-specific-membrane-antigen**

INTRODUCTION

Prostate carcinoma is a common tumor among males in developed countries [1]. In nearly all of these patients, cancer progresses despite initial treatment with surgical or pharmacologic androgen ablation therapy [2]. Managing hormone-refractory prostate carcinoma remains a difficult challenge for the clinician; therefore, new pharmacologic agents are needed to complement established regimens, particularly in cases where surgical and/or medical treatment fail to cure the patients (e.g. relapsing, metastatic disease). Immunotherapy based on immunoconjugates is a new form of treatment targeting neoplastic cells expressing tumor-specific or tumor-associated markers. Cell-selective cytotoxic reagents (Immunotoxins, ITs) can be obtained by linkage of vehicle molecules (e.g., antibodies, ligands, growth factors) recognizing cell

Grant sponsor: AIRC; Grant sponsor: MURST.

*Correspondence to: Marco Colombatti, Section of Immunology, Department of Pathology, University of Verona, c/o Policlinico G.B. Rossi, p.le L.A. Scuro 10, I-37134 Verona, Italy.
E-mail: marco.colombatti@univr.it

Received 8 January 2002; Accepted 26 March 2002
DOI 10.1002/pros.10117

surface structures to potent enzymatic polypeptide toxins (e.g., ricin, diphtheria toxin, *Pseudomonas* exotoxin A) [3,4].

The holotoxin ricin is formed by two subunits held together by a disulfide bridge [3,4]. The A subunit (ricin A-chain, RTA) is an enzyme able to catalytically inactivate the protein synthesis machinery of the target cell by attacking ribosomal RNA [3,4]. The B subunit (ricin B-chain, RTB) binds ubiquitous cell surface structures and facilitates intracellular trafficking and membrane translocation of RTA. The binding/translocation subunit is often replaced by a cell-selective ligand. Several ricin- and RTA-based ITs against various blood-borne as well as solid malignancies have demonstrated potent anti-tumor effects in vitro and in animal models [3,4]. Some of these have already undergone clinical phase I/II trials. ITs-based therapy, thus, is evolving into a separate modality of cancer treatment, capable of rationally targeting cells on the basis of surface markers [5]. Therefore, it is likely that provided operationally selective tumor markers are available, ITs may become a useful complement to other forms of therapy also in prostate cancer, particularly in those instances for which ITs may better display their anti-tumor potential (i.e., in the elimination of small clusters of target tumor cells).

Biomarkers of prostate cancer have been used in screening, diagnosis, and predicting disease progression. Prostate specific membrane antigen (PSMA) is a new marker of prostate cancer originally identified in LNCaP cells by immunoprecipitation with monoclonal antibodies [6]. PSMA is an integral membrane glycoprotein of 100 kDa [6] with folate hydrolase/N-acetylated-alpha linked-acidic dipeptidase (NAALADase) activity [7] and is expressed in normal prostate as well as in a high proportion of prostate carcinomas but is absent from other epithelial tumors [8–11]. Cell surface expression of PSMA is enhanced in higher-grade cancers, metastatic disease, and hormone-refractory prostate carcinoma [10,12–14]. Moreover, PSMA has been found also at the surface of endothelial cells in the neovasculature of tumors but appears to be absent from normal endothelial cells [14–16]. Radioimmunoconjugates of anti-PSMA monoclonal antibody (mAb) are currently used as imaging agents and are being investigated also for radioimmunotherapy in prostate cancer [17,18]. Therefore, PSMA represents an ideal target of macromolecular mAb-based pharmacologic agents. In addition, PSMA is constitutively internalized by the target cell and internalization augments after contact with mAb [19]. This property can be exploited to deliver intracellularly acting cytotoxic agents to target prostate tumor cells. With the present study, we have aimed at a preclinical in vitro characterization of anti-PSMA Immunotoxins to select the most promising IT that might be developed for use in vivo. We herein describe new ITs made with three anti-PSMA mAb (J591, PEQ226.5, and PM2P079.1) linked to the cytotoxin RTA and their cytotoxic effects against $PSMA^+$ target cells. To evaluate the feasibility of targeting three-dimensional (3-D) tumor cell structures, we also used a prostate carcinoma spheroid model. The results obtained warrant further efforts aimed at the development of toxin-based heteroconjugates for in vivo applications in prostate tumors.

MATERIALS AND METHODS

Chemicals and Reagents

All chemicals described were of reagent grade and were purchased from either Sigma (St. Louis, MO) or from Pierce (Rockford, IL). Human diferric Transferrin (Tfn) was obtained from Sigma. Purified mouse anti-human transferrin receptor (TfnR) monoclonal antibody (mAb) OKT9 was obtained previously, as described [20]. Anti-PSMA monoclonal J591 was described elsewhere [19], mAbs PEQ226.5 and PM2P079.1 were supplied by Hybritech (San Diego, CA). Recombinant RTA (rRTA) was produced and purified as previously described [21]. Native RTA (nRTA) isolated to >95% purity from castor beans was generously supplied by Dr. P. Casellas (Sanofi Pasteur, France).

Monolayer Cell Cultures

The LNCaP cell line was used as $PSMA^+$ target of our ITs. LNCaP cells represent the adequate targets for testing ITs against human prostate carcinoma cells, being derived from a $PSMA^+$ human prostate carcinoma explant (American Type Culture Collection, cat. no. CRL-1740). As $PSMA^-$ controls, the following cell lines were used: DU145 ($PSMA^-$ prostate carcinoma), MCF7 (breast carcinoma), and Jurkat (T-cell lymphoblastoma). All cell lines were purchased from the American Type Culture Collection (Rockville, MD) and were maintained in vitro by serial passages in RPMI-10% fetal bovine serum (FBS) at 37°C in a humidified atmosphere of 5% CO_2/95% air. Adherent cells (LNCaP, DU145, and MCF7) were trypsinized (0.05% trypsin in 0.9% NaCl solution, Gibco BRL Life Technologies, Grand Island, NY) before use. Alternatively, adherent cells were detached from plastic surfaces by exposure to ethylenediaminetetraacetic acid (EDTA) 0.02% for 10–15 min at 37°C.

Multicellular Tumor Spheroid Cultures

Spheroids were obtained by inoculating 1.5×10^6 LNCaP cells in 15 ml of RPMI-FBS 10% in Petri dishes (Costar, Cambridge, MA) on a thin layer of agar (10 ml

of a 0.75% solution of agar in RPMI-FBS 10%) following the method described by Yuhas et al. [22]. Spheroids of 125–150 μm diameter (approximately 1,000 cells/spheroid) were harvested with a micropipette and placed in a Petri dish. Single spheroids were then micropipetted into individual wells of a 96-well flat-bottomed microtiter plate on a layer of agar and treated with ITs.

Synthesis of Immunotoxins

Synthesis of Tfn-spdp-nRTA and OKT9-spdp-nRTA conjugates has been described elsewhere [20]. Anti-PSMA Immunotoxins (ITs) were synthesized by chemically cross-linking purified nRTA or rRTA to whole mAb by using N-succinimidyl 3-(2pyridylthio)-propionate (SPDP) or 4-succinimidyloxycarbonyl-alpha- methyl-alpha(2-pyridyldithio)toluene (SMPT) cross-linkers (Pierce), according to described protocols [20]. After derivatization, the mAbs contained 1.5 sulfhydryl groups/antibody molecule, on average. ITs were separated from unconjugated RTA by gel filtration chromatography on a TSK 3000 SW column (Beckman, San Ramon, CA) equilibrated in phosphate buffered saline (PBS) buffer (pH 7.4), and run at 0.5 ml/min by using a fast protein liquid chromatography apparatus (Bio-Rad, Hercules, CA). A further purification from unconjugated antibody was achieved by affinity chromatography on Affi-Blue gel column, as described [20]. The concentration of mAb-bound RTA was determined by a sandwich enzyme-linked immunosorbent assay (ELISA), by using polyclonal goat anti-mouse antibodies as coating reagent and polyclonal rabbit anti-RTA antibodies followed by an alkaline phosphatase-labeled goat anti-rabbit immunoglobulin antiserum as the developing reagent. Titration of RTA was obtained by using known concentrations of OKT9 cross-linked RTA as a standard reference. The concentration of IT is standardized based on the concentration of antibody-bound RTA throughout this study.

mAb Labeling with ^{125}I and Binding of ^{125}I-Labeled mAbs to LNCaP Cells

The mAbs were labeled with ^{125}I (NEN Dupont, Boston, MA) by the Iodo-beads method (Pierce), following the recommendations of the manufacturer. Free ^{125}I was separated from ^{125}I-mAb by two passages onto Micro Bio Spin 6 chromatography columns (Bio-Rad). Specific activity achieved was generally 1.2 μCi/μg protein. Binding of ^{125}I-labeled mAbs was evaluated by incubating 5×10^5 LNCaP cells in 150 μl of PBS-BSA 0.2% with 5 nM radiolabeled mAb mixed with increasing concentrations of cold mAb, as indicated in Figure 1 for 1 hr on ice. The cells were then washed three times with cold PBS-BSA 0.2% to remove unbound ^{125}I-labeled mAb. After the last washing, the cell pellet was counted in a gamma-spectrometer. Raw binding data expressed in counts per minute were processed according to the method of Scatchard [23] to calculate dissociation constant (K_d) and number of binding sites/cell (intercept on the x-axis corresponding to the extrapolated maximum concentration of bound ligand [B_{max}]).

Flow Cytometry

Cells from monolayer cultures were treated with 0.02% EDTA for 10–15 min at 37°C, harvested, washed three times and re-suspended in cold PBS-BSA 0.2% containing saturating amounts of the anti-PSMA or anti-TfnR OKT9 mAb. After 1 hr incubation on ice, the cells were washed with cold PBS and stained with saturating amounts of an anti-mouse immunoglobulin fluorescein isothiocyanate (FITC)-labeled goat antibody (Becton and Dickinson, Sunnyvale, CA). Cell associated fluorescence was then analysed by flow cytometry by using an Epics XL cytometer (Coulter, Hyaleah, FL) equipped with an exciting wavelength of 488 nm at 200 mW power. The percentage of positive cells and the mean fluorescence intensity (MFI) values were considered. For each different mAb under saturating conditions of the first and of the second step antibodies, the MFI value is proportional to the number of Ag sites.

To compare the binding activity of the three anti-PSMA mAbs, LNCaP cells were incubated with serial dilutions of the mAbs under study. Staining and cytofluorometric analysis were then performed as described above. Data are expressed as percentage saturation of the total stainable PSMA sites.

Competitive binding studies were performed by examining the displacement of a fixed amount (10 nM) of biotinylated mAb by using serial threefold dilutions (beginning with a 100-fold excess) of the unmodified antibody under study. mAbs were biotinylated with NHS-d-Biotin (Sigma) following the manufacturer's instructions. The binding of biotinylated mAbs was then detected by a second step labeling carried out with FITC Avidin D (Vector Laboratories, Burlingame, CA) at 10 μg/ml.

To evaluate PSMA and TfnR expression on the surface of cells growing in 3-D cultures, multicellular tumor spheroids (MTS) were harvested from Petri dishes, washed twice by centrifugation, mechanically disaggregated and incubated in EDTA 0.02% for 5 min. After washings, the cells were subjected to staining and flow cytofluorometry as described for monolayer cultures.

Cytotoxicity

IT-mediated cytotoxicity was indirectly evaluated by measuring [^{14}C]leucine or [^{3}H]TdR incorporation in untreated and IT-treated cell cultures.

Monolayer cultures. The cytotoxic effect of the different ITs on monolayer cells was evaluated by measuring cell proliferation. Thirty thousand cells in 50 μl of RPMI-FBS 10% were dispensed in 96-well flat-bottomed microtitration plates. Ten-fold dilutions of ITs in 10 μl of PBS-BSA 0.2% were then added followed by 40 μl of RPMI-FBS 10%. Microcultures were then incubated for 24 hr. After this time, the cells were pulsed for 8 hr with 1 μCi [methyl-^{3}H]thymidine (6.7 Ci/mmol) (NEN DuPont). At the end of the assay, the cells were harvested onto glass-fiber filters, washed with water, and dried. Radioactivity incorporated by the cells was then measured in a beta-spectrometer. Results are expressed as a percentage of the incorporation of control mock-treated cultures. The cytotoxic activity of different reagents was compared by considering their IC_{50} values, corresponding to the concentrations needed to reduce the cell proliferation of target cells by 50%. The average ± SD of 4–5 experiments by using LNCaP cells is shown. The nonspecific effects of ITs treatment were evaluated on $PSMA^{-}$ cell lines by using the same procedures described above. Representative experiments conducted by using $PSMA^{-}$ cell lines are shown.

The ratio IC_{50} of RTA/IC_{50} of the IT is defined as ''Potentiation'' and represents the increase in cytotoxicity obtained by conjugating RTA to a vehicle molecule. The ratio of the IC_{50} observed in $PSMA^{-}$ cell lines and the IC_{50} observed in $PSMA^{+}$ LNCaP cells offers a measure of the specificity of the anti-PSMA ITs and is defined by the term ''Specificity window.''

To investigate the possible interference of serum-derived factors with anti-PSMA ITs-mediated cytotoxicity, assays were conducted in the presence of serum obtained from patients affected by prostate carcinoma. Selected patients had not received prior treatment and were categorized from grade 5 to 9 according to Gleason grading system. Histologic examination revealed that tumors of the patients were all scarcely differentiated. Trace amounts of PSMA were evidenced in the patients' sera by Western blotting (not shown). LNCaP cells in 96-well plates were incubated in 100% serum from each patient separately for 12 hr at 37°C in the presence of various doses of J591-smpt-nRTA. As a control, LNCaP cells were treated for the same time in RPMI-FBS 10% or in the presence of 100% serum from normal male or female volunteer donors. After exposure to anti-PSMA Its, the medium was replaced with RPMI-FBS 10% and the cells cultured for a further 12 hr. The cells were then pulsed for 8 hr with 1 μCi [methyl-^{3}H]thymidine and cell proliferation was measured as described above.

Kinetics of cytotoxicity assays were performed under the same general conditions as described for the dose-response assays. The length of the treatment with ricin and ITs ranged from 3 to 48 hr. L-[^{14}C]leucine (1 μCi, 315.6 mCi/mmol) (NEN DuPont) was added during the last 2 hr of the treatment. In kinetics experiments, the ITs were used at concentrations yielding similar effects in dose-response assays (79.2 ng/ml, 540 ng/ml, 4.7 μg/ml, 1.1μg/ml, and 130 pg/ml for J591-smpt-nRTA, PEQ226.5-spdp-nRTA, PM2P079.1-spdp-nRTA, Tfn-spdp-nRTA, and ricin, respectively, see also Table IV). Protein synthesis inactivation by ITs is first order with time [24]. The plot of the percentage protein synthesis vs. time on a semilog diagram is, therefore, a straight line. The slope of the linear curve represents the first-order constant of the process; under these conditions the rate of protein synthesis $(S) = e^{-kt}$($\ln S = -kt$), where k is the slope of the curve, and t is the time. K is the first-order rate constant at concentrations below receptor saturation. The kinetics of cytotoxicity of different ITs were compared on the basis of the time required to inhibit 90% protein synthesis (T_{10}) values [25]. T_{10} represents the time required to reduce the protein synthesis by 1 order of magnitude (1 log kill, corresponding to the elimination of 90% target cells). The T_{10} does not consider the lag time.

Spheroids. Groups of 15–20 MTS were individually treated with different doses of ITs, nRTA, or mAb J591 alone, in the wells of flat-bottomed 96-well plates in a total volume of 100 μl on a thin layer of agar. The ITs, nRTA, or mAb J591 were omitted from the medium of control mock-treated MTS and replaced with PBS-BSA 0.2%. After 32 hr of treatment, the IT-containing medium was replaced by fresh RPMI-FBS 10% by gentle repeated transfer of individual spheroids into the wells of a 24-well culture plate (Costar); MTS were then placed into the wells of a 24-well plate containing 1 ml of RPMI-FBS 10% on a layer of 0.5 ml agar. The longest spheroid diameter (D) and the perpendicular diameter (d) were measured by using a calibrated ocular micrometer on an inverted microscope. The volume (V) was calculated according to the formula $V = 4/3\pi r^3$, where $r = (Dd)^{1/2}/2$ is the mean radius of the spheroid. The growth kinetics of treated and control spheroids was followed for 50–55 days. The time ''0 days'' in Figure 7 corresponds to the time immediately after treatments. Individual growth curves were fitted by the Gompertz growth equation $V_t = V_0\exp\{\alpha/\beta[1\text{-}\exp(-\beta t)]\}$ where V_t is the volume of

the spheroid at time t, V_0 is the initial volume, α is the instantaneous growth rate, and β is the retarding factor. The best fits were performed by using a least-square estimation algorithm [26]. The computer output also yielded the following quantities, whose values were taken to evaluate the goodness of the nonlinear curve fitting according to widely accepted criteria (reviewed in Landaw and Distefano [27]): the standard error (SE) and generalised Student *t*-value for each parameter; the multiple correlation coefficient; variance-covariance matrix; and correlation matrix. Curve fitting was considered acceptable in 99% of analyzed MTS.

The cytoreductive effects of ITs and of nRTA on MTS could be measured only in spheroids displaying a measurable regrowth curve after a delay. Experimental data of volume increase vs. time were fitted with the Gompertz growth equation and suitable regrowth curves were extrapolated backward to the time immediately after treatment (0 days). The corresponding ordinate at time ''0 days'' was taken as the volume of the spheroid after a given treatment (V_{tr}) [20,28]. The surviving fraction of cells escaping treatment (F) was then calculated by using the formula [28]: $F = V_{tr}/V_{ctrl}$, where V_{ctrl} is the volume of control mock-treated MTS at time 0 days. The log kill for each treatment could then be derived as follows [20,28]: log kill $= -\log(F)$.

MTS that survived treatment with 6.3 ng/ml J591-smpt-nRTA and re-grew after a delay were harvested when they reached a volume of approximately 1,000 μm, disaggregated and the isolated cells were washed. The monocellular suspension was then plated in tissue culture flasks in the absence of agar. Cells were let to expand in culture for 20 days, the cells were then harvested, re-plated in 96-well microtiters and exposed to J591-smpt-nRTA at different doses for 32 hr. Cell proliferation was then measured at the end of the assay.

RESULTS

Binding of Anti-PSMA mAb to Cells from Monolayers or from MTS

The binding properties of anti-PSMA mAbs were studied by radioimmunoassay and by flow cytofluorometry.

Radioimmunoassay. The saturation binding curves obtained with ^{125}I-labeled mAbs (Fig. 1) and the data elaboration according to Scatchard (Fig. 1, inset) are characteristic of binding to a single class of sites. The values of K_d observed demonstrated that the three mAbs bound the cells with different affinity (K_d was 15.3 ± 2.9 nM, 9.3 ± 4.2 nM, and 74.5 ± 19.7 nM, for mAb J591, PEQ226.5, and PM2P079.1, respectively).

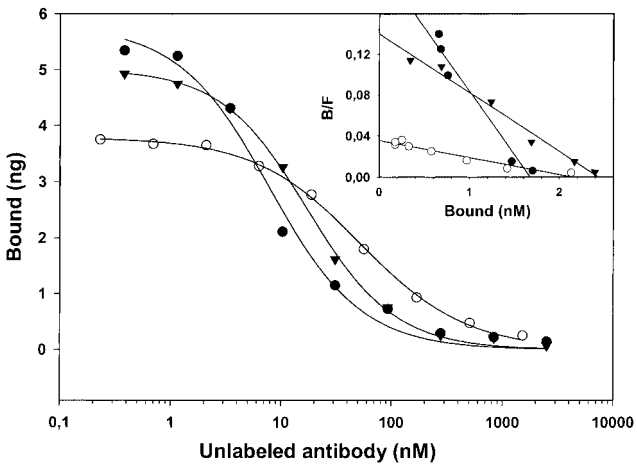

Fig. 1. Binding plot (best fit) of mAb J591 (triangles), PEQ226.5 (filled circles), and PM2P079.1 (open circles). Shown is the binding of 5nM radiolabeled monoclonal antibody (mAb) in the presence of increasing concentrations of cold mAb. Inset: Scatchard plot transform of data in the figure.

The value of K_d observed for mAb J591 is higher than that reported by McDevitt et al. (i.e., 3 nM) [18]. This difference, however, might be attributed to differences in the labeling protocol, in the assay procedure and/or in data analysis. The number of sites bound/cell by the three mAbs, as calculated based on the intercept with the x-axis (B_{max} in a Scatchard plot) (Fig. 1, inset) was $240{,}000 \pm 130{,}000$ (J591), $330{,}000 \pm 150{,}000$ (PEQ226.5), and $450{,}000 \pm 80{,}000$ (PM2P079.1).

Flow cytofluorometry. Radioimmunoassays do not allow evaluation of cell surface Ag distribution in a cell population nor do they allow discrimination between viable and dying cells. Cell surface expression of PSMA and binding of anti-PSMA mAb, therefore, was evaluated also by indirect immunofluorescence and flow cytofluorometry by using $PSMA^+$ and $PSMA^-$ cells as targets. It can be observed (Table I) that all anti-PSMA mAbs stain LNCaP cells (percentage of positive cells in monolayer cultures ranging from 95.9% to 97.2%). The shape of the curves of fluorescence vs. number of events suggested that PSMA is homogeneously distributed within the LNCaP cell population. As a comparison, cell samples were also labeled with the anti-TfnR mAb OKT9. As shown in Table I, LNCaP cells were 95.2% $OKT9^+$ with a lower antigen density compared with mAbs J591 and PEQ226.5.

To evaluate the specificity of binding of the anti-PSMA mAbs under investigation, $PSMA^-$ target cells were also stained and analyzed by flow cytofluorometry. As shown in Table I, the mAbs J591, PEQ 226.5, and PM2P079.1 do not stain the $PSMA^-$ cells considered by us (percentage of positive cells ranging from 0.02% to 0.46%).

TABLE I. Staining of PSMA$^+$ and PSMA$^-$ Cell Lines by Anti-PSMA Monoclonal Antibodies*

	PSMA$^+$ cells		PSMA$^-$ cells		
Monoclonal	LNCaP[a] monolayer	LNCaP MTS	DU 145	MCF7	Jurkat
J591	96.7 (16.2)[b]	98.6 (15.7)	0.46	0.1	0.08
PEQ226.5	97.2 (14)	98.4 (13.5)	0.02	0.22	0.07
PM2P079.1	n.d.	n.d.	0.23	0.21	0.04
OKT9	95.2 (8.2)	96.4 (6.6)	96.7 (16.8)	95 (4.5)	98.9 (15.4)
J591-smpt	96.4 (15)		0.59	0.1	0.08
PEQ226.5-spdp	93.7 (9.1)		0.84	0.55	0.09
PM2P079.1-spdp	94.5 (n.d.)		1.51	2	0.04

*PSMA, prostate specific membrane antigen; n.d., not determined.
[a]Cells were analyzed by indirect immunofluorescence and flow cytofluorometry (see Materials and Methods section).
[b]Values represent the percentage of positive cells. Numbers in brackets represent the mean fluorescence intensity values. Background (staining with fluoresceinated goat anti-mouse immunoglobulin antibody alone) is subtracted.

The binding properties of mAbs J591, PEQ 226.5, and PM2P079.1 were compared by treating LNCaP cells with increasing concentrations of the first step anti-PSMA mAb followed by incubation with a saturating amount of a second step FITC-labeled goat antibody followed by cytofluorometric analysis. The results obtained were similar to those obtained by radioimmunoassay (Fig. 2). In particular, the mAb PEQ226.5 appears to reach saturation of PSMA sites at the lowest concentration of 4 nM, whereas J591 and PM2P-079.1 showed an intermediate binding activity, reaching 50% saturation of PSMA sites at approximately 11 nM and 28 nM, respectively.

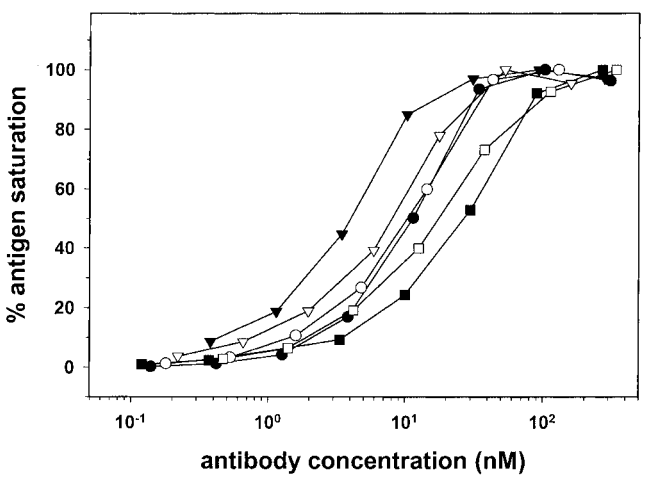

Fig. 2. Binding of unmodified (filled symbols) and derivatized (open symbols) anti–prostate specific membrane antigen monoclonal antibodies (mAb) to LNCaP cells. Cells were incubated with mAb J591 (circles), PEQ226.5 (triangles), or PM2P079.1 (squares), washed to eliminate unbound antibody, and stained with a fluorescein isothiocyanate–labeled goat anti-mouse immunoglobulin antiserum.

Effect of derivatization with SMPT or SPDP. The effect of derivatization on the binding properties of the three mAbs was also investigated by flow cytofluorometry. As illustrated in Figure 2, mAb J591 was not affected by SMPT derivatization because the binding of unmodified and SMPT-derivatized J591 was identical. The binding of mAb PM2P079.1 was slightly ameliorated by derivatization with the cross-linker SPDP, whereas mAb PEQ 226.5 showed a moderate reduction in binding after SPDP derivatization (50% saturation of PSMA sites at 4 nM before and at 8 nM after derivatization with SPDP). The effect of derivatization on mAb specificity was also evaluated. PSMA$^-$ cells, therefore, were incubated with anti-PSMA mAbs followed by a second-step fluoresceinated anti-mouse antibody and analyzed by cytofluorometry. As illustrated in Table I, it can be observed that derivatized anti-PSMA mAbs did not recognize PSMA$^-$ cells (percentage of positive cells ranging from 0.04% to 2%).

Competitive binding. Competitive binding of the three anti-PSMA mAbs was investigated by displacing biotinylated mAb with unmodified mAbs used as competitors. The binding of the biotinylated mAb was revealed by fluoresceinated avidin. As shown in Figure 3, the two mAbs J591 and PEQ226.5 were able to cross-inhibit the binding of each other, whereas the mAb PM2P079.1 could not out compete the binding of either J591 or PEQ226.5 and its binding to the cell surface was in turn not inhibited by the other two mAbs. The epitope recognized by PEQ226.5 has been

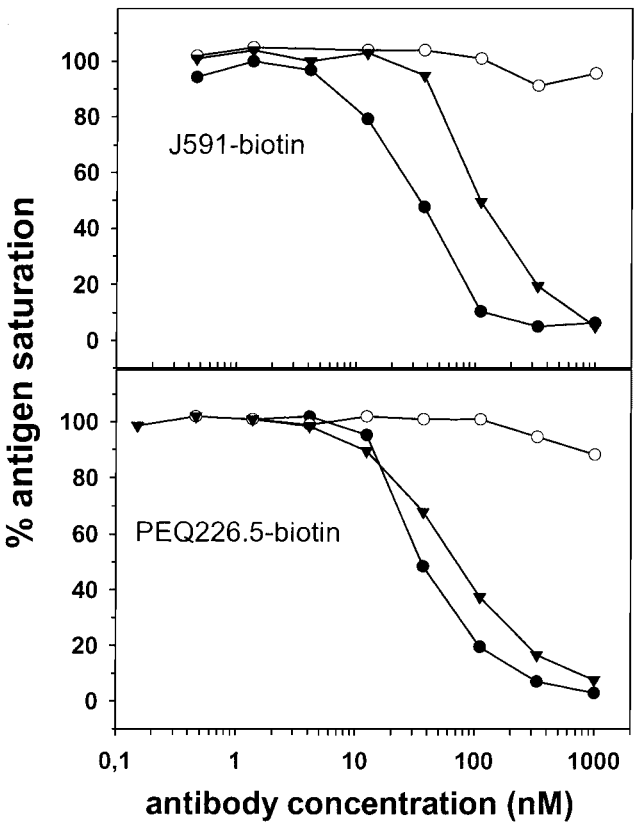

Fig. 3. Upper panel: displacement binding of a fixed amount of J591-biotin (10 nM) with unmodified mAb J591 (triangles), PEQ226.5 (filled circles), or PM2P079.1 (open circles), at the concentrations reported on the x-axis. Lower panel: displacement binding of a fixed amount of PEQ226.5 (10 nM) with unmodified mAb J591 (triangles), PEQ226.5 (closed circles), or PM2P079.1 (open circles), at the concentrations reported on the x-axis.

mapped within the segment between amino acids 134 and 437 of the PSMA molecule [29]. Therefore, it is likely that mAbs J591 and PEQ226.5 recognize the same epitope or epitopes that are physically or functionally associated in the PSMA molecule. The epitope recognized by mAb PM2P079.1 is probably not related to the ones recognized by the other two mAbs.

Expression of PSMA in MTS. To estimate PSMA expression in LNCaP cells forming MTS, a pool of spheroids of various sizes (range, 240–350 μm diameter) were harvested, a monocellular suspension was obtained, and single cells were analyzed by cytofluorometry. As shown in Table I, the percentage of positive cells was comparable to that observed in monolayer cells. The PSMA sites density (as assessed by MFI) in LNCaP monolayers and MTS was also comparable, indicating that a 3-D organization did not lead to down-regulation of PSMA at the cell surface. Expression of TfnR was instead approximately 20% lower in MTS compared with monolayer cultures (Table I).

Effect of Anti-PSMA Imunotoxins in Cell Monolayers

Cytotoxicity. To evaluate the cytotoxic effect of anti-PSMA ITs, we measured the proliferation of $PSMA^+$ and $PSMA^-$ target cells treated with ITs in dose-response assays. Figure 4 shows the results of a typical experiment, whereas Tables II and III summarize a larger set of results obtained in experiments conducted under various conditions. As illustrated in Table II and Figure 4, of the various ITs assayed, J591-smpt-nRTA and J591-smpt-rRTA showed the highest cytotoxic activity against $PSMA^+$ LNCaP cells ($C_{50} = 1.6 \pm 0.7$ ng/ml and 1.8 ± 0.4, respectively). The IT PEQ226.5-spdp-nRTA showed instead a lower cytotoxic activity ($IC_{50} = 10.1 \pm 2.9$ ng/ml), and the IT PM2P079.1-spdp-nRTA showed the lowest cytotoxicity of the three ITs ($IC_{50} = 99 \pm 23.2$ ng/ml).

The cytotoxic effects of the various anti-PSMA ITs were then compared with those displayed by whole ricin, nRTA, and heteroconjugates directed against the TfnR, whose physiology and ability to mediate ITs internalization and cytotoxicity are well known [30–33]. Although the cytotoxic activity of the three anti-PSMA ITs examined was found to be much lower than that of the holotoxin ricin ($IC_{50} = 3.3 \pm 3$ pg/ml), their cytotoxic potency was considerably greater than that shown by the isolated nRTA or rRTA (Table II). Therefore, it appeared that the cross-linking of the three anti-PSMA mAbs to RTA could substantially potentiate the toxicity of RTA against target cells. In fact, as shown in Table II (see Potentiation column),

TABLE II. Effect of Immunotoxins on $PSMA^+$ LNCaP Cells*

Immunotoxin/toxin	IC_{50}	Potentiation
J591-smpt-nRTA	1.6 ± 0.7	5,208
J591-smpt-rRTA	1.8 ± 0.4	3,528
PEQ226.5-spdp-nRTA	10.1 ± 2.9	825
PEQ226.5-smpt-nRTA	12 ± 1.3	694
PEQ226.5-spdp-rRTA	24.2 ± 5.7	262
PM2P079.1-spdp-nRTA	99 ± 23.2	84.2
Tfn-spdp-nRTA	47.5 ± 10.6	175
OKT9-spdp-nRTA	21 ± 1.4	397
Ricin	$3.3 \times 10^{-3} \pm 3 \times 10^{-4}$	2.5×10^6
nRTA	$8{,}333 \pm 1{,}154$	1
rRTA	$6{,}350 \pm 1{,}527$	1

*IC_{50} is the concentration (ng/ml) of the immunotoxin/toxin inhibiting 50% cell proliferation. Potentiation represents the increase of cytotoxicity achieved by conjugation of RTA to a vehicle molecule, calculated according to the formula IC_{50} of RTA/IC_{50} of the immunotoxin. PSMA, prostate specific membrane antigen; RTA, ricin A-chain.

TABLE III. Effect of Immunotoxins on PSMA$^+$ and PSMA$^-$ Cell Lines*

Immunotoxin/toxin	LNCaP	Du145	MCF7	Jurkat	Specificity window
	IC_{50}				
J591-smpt-nRTA	1.6[a]	200	126	100	62 ÷ 125
PEQ226.5-pdp-nRTA	10.1	2,800	1,800	2,100	178 ÷ 277
PM2P079.1-spdp-RTA	99	20,000	8,000	7,500	76 ÷ 202
Tfn-spdp-nRTA	47.5	9.9	9	2.2	
Ricin	3.3×10^{-3}	0.1	0.12	0.015	
nRTA	8,333	10,000	4,000	7,000	

*The Specificity window represents the difference in cytotoxic effect of anti-PSMA ITs observed in PSMA$^-$ cell lines vs. that observed in PSMA$^+$ LNCaP cells, according to the formula: IC_{50} obtained in the PSMA$^-$ cell line under investigation/IC_{50} obtained in LNCaP cells. PSMA, prostate specific membrane antigen; nRTA, native ricin A-chain; ITs, Immunotoixins; IC_{50}, concentration inhibiting 50% cell proliferation or protein synthesis.
[a]Values are those of Table II, reported here for ease of comparison. Numbers represent IC_{50} values (ng/ml).

the increase of nRTA/rRTA cytotoxicity is between 5208-fold and 84-fold, after conjugation to anti-PSMA mAbs. The unconjugated anti-PSMA mAbs had no measurable cytotoxic effects against LNCaP cells at the concentrations assayed (range, 50 ng/ml to 50 μg/ml) (not shown). Moreover the ITs J591-smpt-nRTA and PEQ226.5-spdp-nRTA were even more effective than RTA-based anti-TfnR heteroconjugates which showed an IC_{50} of 47.5 ± 10.6 ng/ml (Tfn-spdp-nRTA) and 21 ± 1.4 ng/ml (OKT9-spdp-nRTA) (Table II).

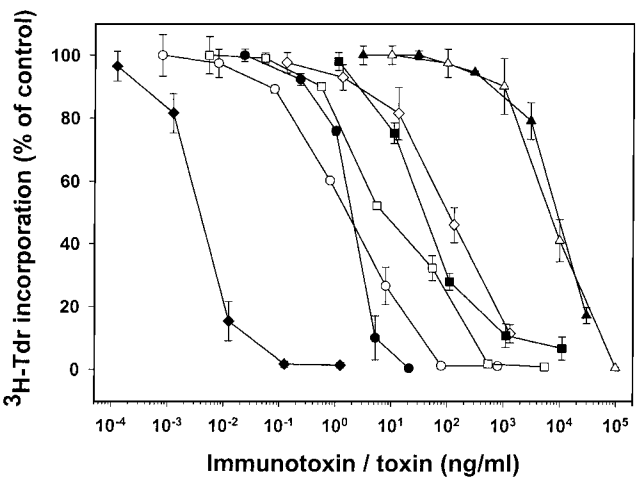

Fig. 4. Effect of treatment of LNCaP cells monolayers with ricin (filled diamonds), native ricin A-chain (nRTA; filled triangles), recombinant RTA (rRTA; open triangles), J591-smpt-nRTA (open circles), J591-smpt-rRTA (filled circles), PEQ226.5-spdp-nRTA (open squares), PM2P079.1-spdp-nRTA (open diamonds), or Tfn-spdp-nRTA (filled squares). Cells were exposed to the various reagents for 32 hr.

Role of cross-linkers. The mAb J591 is being investigated for possible applications in radioimmunotherapy in humans [34]. The cross-linker SMPT, therefore, was used to synthesize the IT J591-smpt-nRTA, because it shows higher in vivo stability and might be better suited for making ITs that are to be applied in the clinics [35,36]. To investigate the influence of different cross-linkers on the cytotoxic activity of our ITs, we compared the cytotoxicity of ITs prepared with either SPDP or SMPT. As shown in Table II, we found that the cytotoxicity of the IT PEQ226.5-spdp-nRTA and that of the IT PEQ226.5-smpt-nRTA were almost superimposable (IC_{50} of 10.1 ± 2.9 ng/ml and 12 ± 1.3 ng/ml, respectively), thus demonstrating that the choice of the cross-linker had no influence on the overall activity of anti-PSMA ITs assayed in vitro and that results obtained with SPDP cross-linked ITs can be extrapolated to SMPT cross-linked heteroconjugates.

Native and recombinant RTA. nRTA is endowed with high mannose residues that might interact in vivo with target cells bearing mannose receptors, contributing to higher nonspecific toxicity and side effects [37,38]. For this reason, use of rRTA would be preferable in vivo. To make sure that our in vitro results were not affected by the use of either form of RTA, we compared the cytotoxicity of ITs made linking J591 and PEQ226.5 mAbs to nRTA or rRTA. We could observe no differences in cytotoxicity between J591-smpt-nRTA and J591-smpt-rRTA (Fig. 4; Table II), but we did observe a twofold difference in cytotoxic potency between PEQ226.5-spdp-nRTA and PEQ226.5-spdp-rRTA ($IC_{50} = 10.1 \pm 2.9$ ng/ml and 24.2 ± 5.7 ng/ml, respectively, Table II). Although this small difference may not influence the end results of in vivo

treatments, particularly considering that these reagents are effective over wide range of concentrations, we decided to make sure that even this small difference in IC_{50} was not due to endocytosis by means of mannose receptors and compared the killing efficacy of rRTA and nRTA in the presence or in the absence of 0.1 M mannose, known to inhibit binding of RTA to cells by means of the mannose receptor [39]. The results did not evidence a meaningful difference in cytotoxicity (not shown), thus ruling out that the different IC_{50s} of PEQ226.5-spdp-nRTA and of PEQ226.5-spdp-rRTA could be due to mannose receptors-mediated endocytosis.

Specificity. The specificity of IT-mediated cell killing was investigated by comparing the effects of the three ITs in $PSMA^+$ and $PSMA^-$ cells. As illustrated in Table III the three $PSMA^-$ cell lines used were 62- to 125-fold less sensitive to J591-smpt-nRTA, 178- to 277-fold less sensitive to the IT PEQ226.5-spdp-nRTA, and 76- to 202-fold less sensitive to the IT PM2P079.1-spdp-nRTA (see Specificity window column, Table III). The three $PSMA^-$ target cells, however, showed sensitivity to RTA similar to the $PSMA^+$ LNCaP cells and were somewhat more sensitive to the control heteroconjugate Tfn-spdp-nRTA, thus demonstrating that the reduced cytotoxic effect of anti-PSMA ITs is not due to a lower intrinsic sensitivity to the toxin or to internalized heteroconjugates. As a further specificity control, we also incubated LNCaP target cells with anti-PSMA ITs in the presence of a 100-fold excess unconjugated mAb, to displace IT binding and specifically prevent cytotoxicity. We found that, by co-incubation with the relevant unconjugated mAbs, the cytotoxic effect of the ITs J591-smpt-nRTA, PEQ226.5-spdp-nRTA, and PM2P079.1-spdp-nRTA was diminished by approximately 100-fold in all cases, thus demonstrating that the killing of $PSMA^+$ LNCaP cells was indeed specific and Ab-mediated.

Effect of serum from prostate carcinoma patients. Substances present in the serum of normal subjects or in the serum of patients affected by prostate carcinoma could inhibit/inactivate anti-PSMA ITs or interfere with the cell intoxication process. To investigate this aspect, LNCaP cells were exposed to J591-smpt-nRTA in the presence of serum obtained from patients. For these experiments, we selected the IT J591-nRTA where the mAb J591 is cross-linked to native glycosylated RTA, because the presence of sugar residues on RTA molecule may allow greater interactions with serum-derived proteins and could maximize the possible blocking effects of serum factors [3,4]. Figure 5 shows the dose-response curves of cytotoxicity obtained in the presence or in the absence

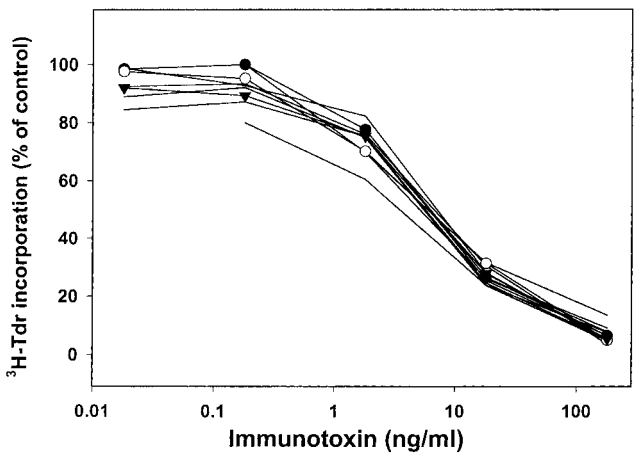

Fig. 5. Effect of treatment of LNCaP cells in the absence (open circles) or in the presence (filled circles) of serum from normal male, normal female (triangles), or prostate cancer patients (no symbols). Curves represent results obtained with serum from individual patients. Target cells were exposed to the indicated concentrations of J591-smpt-nRTA for 12 hr, the cells were then washed and further cultured for a total time of 32 hr.

of serum. The average IC_{50} in the presence of patients' serum was 5.45 ± 1.9 ng/ml, and the IC_{50} of the control sample treated in the absence of serum was 3.6 ng/ml, showing that the presence of serum has only scarcely appreciable effects on the overall cytotoxic potential of the anti-PSMA ITs. Effects of J591-smpt-nRTA in the presence of control serum from a normal male and a normal female subjects were comparable (Fig. 5). Slightly lower IC_{50s} were observed in this assay as compared with those reported in Table II due to shorter target cell treatment. Shown in Figure 5 are data obtained with sera from nine patients.

Kinetics of cell intoxication. Anti-PSMA mAbs are rapidly internalized. Toxin- and IT-mediated protein synthesis inactivation follows a first-order kinetics, and measurements of cell killing kinetics may supply useful information concerning the cytoreductive potential of an IT [24,40,41]. Moreover, fast-acting ITs are preferable, because they may kill a larger burden of target cells in a shorter time [24,40,41]; therefore, we have conducted kinetic assays of protein synthesis inhibition and compared the effects of J591-smpt-nRTA, PEQ226.5-spdp-nRTA, PM2P079.1-spdp-nRTA, and Tfn-spdp-nRTA taken at concentrations resulting in comparable effects in dose-response assays (Table IV). Ricin was used as a reference standard and the following parameters were considered: (1) the lag phase (i.e., the time elapsing before protein synthesis inhibition can be measured), which is related to intracellular processing events preceding the translocation of the toxic component to the cytosol of the target cell; and (2) the T_{10}, which is the time needed to inhibit

TABLE IV. Kinetic Parameters of Cell Killing by Anti-PSMA Immunotoxin in LNCaP Monolayers*

Immunotoxin/toxin	Concentration (ng/ml)	% Protein synthesis	Lag phase (min)	T_{10} (min)
J591-smpt-nRTA	79.2	1.1	200	625
PEQ226.5-spdp-nRTA	540	1.8	280	1,333
PM2P079.1-spdp-nRTA	4,700	3	308	1,622
Tfn-spdp-nRTA	1,100	8	247	1,765
Ricin	0.13	1	57	249

*Residual protein synthesis measured in a 32-hr assay at the concentration indicated in the previous column. The T_{10} represents the time required to reduce the rate of protein synthesis by 1 order of magnitude (1 log kill). PSMA, prostate specific membrane antigen; nRTA, native ricin A-chain.

protein synthesis in 90% of the target cells. As shown in Figure 6 and summarized in Table IV, J591-smpt-nRTA displays the shortest lag phase (200 min), after this time inhibition of protein synthesis begins with a T_{10} of 625 min. The other heteroconjugates perform less well than J591-smpt-nRTA, showing longer lag phases (280 min, 308 min, and 247 min, for PEQ226.5-spdp-nRTA, PM2P079.1-spdp-nRTA, and Tfn-spdp-nRTA, respectively), and longer T_{10s} (1,333 min, 1,622 min, and 1,765 min, for PEQ226.5-spdp-nRTA, PM2P079.1-spdp-nRTA, and Tfn-spdp-nRTA, respectively). Moreover, these effects are reached at higher concentrations than J591-smpt-nRTA (Table IV).

Effects of Anti-PSMA Immunotoxins on Multicellular Tumor Spheroids

The growth kinetics of treated and control mock-treated LNCaP MTS was evaluated. Figure 7 shows the results of treatments with different concentrations of the IT J591-smpt-nRTA. Table V summarizes the results of experiments performed with LNCaP MTS where also the effects of Tfn-spdp-nRTA, nRTA, and mAb J591 alone were considered. Treatment was carried out when MTS reached 125–150 μm diameter, which corresponds to approximately 1,000 cells/spheroid [34,42]. Control MTS grew after Gompertzian kinetics and their growth parameters (α, β, V_0, doubling time) are comparable to those already reported for LNCaP MTS [34,42]. Treated MTS displayed instead heterogeneous growth behavior depending on the IT concentration used. Two patterns of altered growth kinetics were observed at different doses of IT: at the higher concentration, the growth of MTS was completely inhibited (i.e., at 31.7 ng/ml J591-smpt-nRTA, Fig. 7; Table V). To make sure that no surviving target cells could originate a new micromass after a long delay, after 30 days we plated MTS treated at the higher concentrations and which showed no sign of volume increase (Fig. 7) and placed them in plates without agar to allow migration of surviving cells

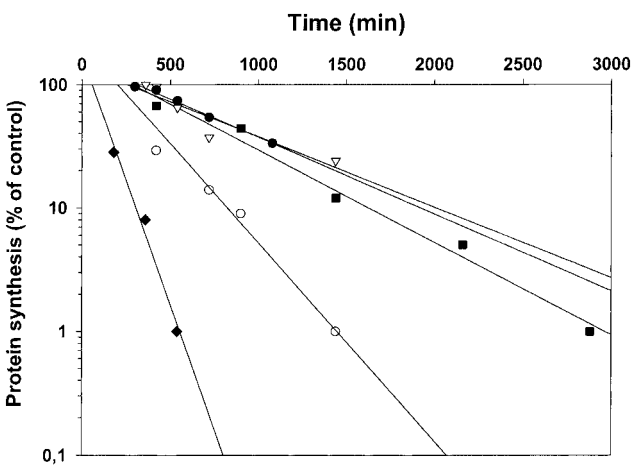

Fig. 6. Kinetics of LNCaP intoxication by ricin (diamonds), J591-smpt-nRTA (open circles), PEQ226.5-spdp-nRTA (squares), PM2P079.1-spdp-nRTA (filled circles), or Tfn-spdp-nRTA (triangles). nRTA, native ricin A-chain.

TABLE V. Cytoreductive Effects of Anti-PSMA ITs in MTS*

Immunotoxin/ toxin	Concentration (ng/ml)	Log kill	% Cells eliminated
J591-smpt-nRTA	31.7	Sterlized	
J591-smpt-nRTA	6.3	1.46	94
J591-smpt-nRTA	0.32	0.35	32
Tfn-spdp-nRTA	110	Sterlized	
Tfn-spdp-nRTA	11	0.89	80
nRTA	30	0.09	8

*Log kill is calculated as described in the Materials and Methods section. PSMA, prostate specific membrane antigen; ITs, Immunotoxins, MTS, multicellular tumor spheroids; nRTA, native ricin A-Chain.

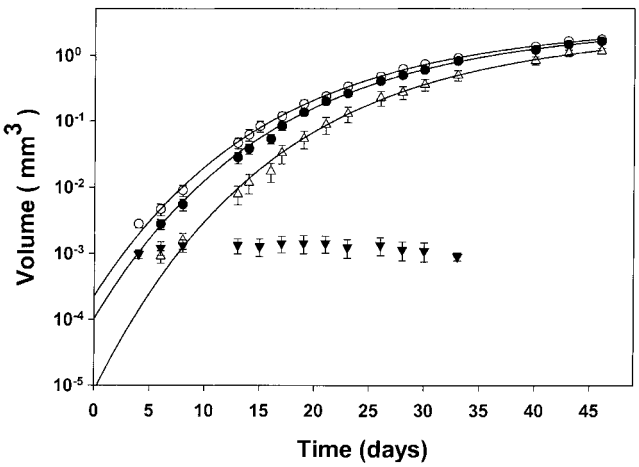

Fig. 7. Effects of treatment with 0.32 ng/ml (filled circles), 6.3 ng/ml (open triangles), or 31.7 ng/ml (filled triangles) of J591-smpt-nRTA on multicellular tumor spheroids (MTS) growth kinetics. Growth of control mock-treated MTS is represented by open circles. Data are expressed as averaged volume increase of a population of treated and control MTS vs. time. Growth curves represent fittings through data points obtained by applying the Gompertz growth equation. nRTA, native ricin A-chain.

outside the MTS and repopulation of the culture wells. However, we could not observe any viable cell up to 30 days after reseeding treated MTS. Therefore, it appears that treatment at the higher concentrations used was effective in eradicating all cells endowed with proliferating potential in the population forming the treated MTS. At lower concentrations of the IT, the growth of treated spheroids showed a dose-dependent delay, after which they resumed Gompertzian growth kinetics (Fig. 7). By considering the Gompertzian parameters α and β, the effect of the treatment could be calculated in terms of log kill [43]. We found that 0.32 ng/ml J591-smpt-nRTA could eradicate 0.35 logs of target cells, whereas 6.3 ng/ml J591-smpt-nRTA achieved a log kill of 1.45 (Fig. 7; Table V), resulting in the eradication of 30% and 95% target cells, respectively. A control heteroconjugate (Tfn-spdp-nRTA) was able to sterilize MTS at 110 ng/ml and achieved a log kill of 0.89 (i.e., 80% cell eradication) at 11 ng/ml. Use of nRTA at 30 ng/ml resulted only in a 0.09 log kill effect (i.e., 8% cell elimination). The observations that MTS re-growing after treatment did so following a Gompertzian pattern and that the calculated doubling times of cells from control or treated MTS were comparable (not shown) indicated that selection of cell subpopulations in IT-treated MTS was unlikely to have occurred.

To determine whether MTS cells surviving treatment could develop resistance to anti-PSMA ITs, MTS treated with 6.3 ng/ml J591-smpt-nRTA showing regrowth after a delay were harvested and disaggregated when they reached 1,000 μm diameter, cells were placed in culture wells without agar, let to expand in culture for 20 days and re-treated as a monolayer with various amounts of J591-smpt-nRTA. Under these conditions, LNCaP cells were as sensitive to J591-smpt-nRTA as the original monolayer cells (average IC_{50} obtained in seven MTS-derived cultures $=2.9 \pm 0.0$ ng/ml).

DISCUSSION

Cytotoxicity

To evaluate the feasibility of eradicating prostate tumor target cells by using mAb-toxin heteroconjugates, we have here conducted a preclinical investigation on the properties and the cytocidal potential of anti-PSMA ITs. The unconjugated mAbs used are not cytotoxic against a $PSMA^+$ prostate tumor cell line but do acquire potent cytotoxic effects when chemically cross-linked to the enzymatic cytotoxin RTA. The ITs obtained are effective in the nanomolar range, thus ranking high among the numerous ITs reported so far [3,4]. Anti-PSMA ITs are in fact 2–3 orders of magnitude more cytotoxic than isolated RTA against LNCaP target cells. However, we observed differences in the cytotoxic potential of the three ITs. In fact, PEQ226.5-spdp-nRTA and PM2P079.1-spdp-nRTA showed a 6.3- and 61.8-fold lower potency compared with J591-smpt-nRTA. These differences could be ascribed to several factors: (1) derivatization with the cross-linker, (2) steric hindrance by cross-linked RTA, (3) PSMA epitope recognized, (4) affinity of the mAb. The mAb J591 is presently being investigated as a promising reagent for use in vivo [34]. For this reason, we have studied in vitro J591-RTA conjugates where mAb J591 is cross-linked to RTA by means of the in vivo stable SMPT bifunctional cross-linker. Our experiments demonstrate that results obtained in vitro with SPDP- and SMPT-derivatized anti-PSMA mAb are comparable. Also nRTA and rRTA appear to be interchangeable in vitro. Nevertheless use of rRTA is recommended in vivo, due to its lack of sugar residues involved in binding to nontarget cells.

Specificity

Evaluation of the cytotoxic effects of the anti-PSMA ITs against $PSMA^-$ cells demonstrated that the original PSMA specificity of the three mAbs was retained after derivatization and cross-linkage to RTA. The specificity window observed in our experiments appears to be promising for use in vivo. Nevertheless, although data from our experiments demonstrate that cell killing by anti-PSMA ITs is selective in vitro,

specificity of the ITs needs to be investigated also in in vivo models. Regrettably, however, such questions can hardly be approached in available murine models, because the anti-PSMA mAbs used by us do not cross-react with the mouse homologue (G. Fracasso et al., personal observation); moreover, enzymatic activity attributable to the human PSMA-like murine homologue is not found in the prostate but primarily in the brain and kidney [44].

Kinetics of Cell Intoxication

Anti-PSMA ITs kill cells with fast kinetics. This phenomenon might be attributable to PSMA physiology and intracellular routing. Upon internalization, PSMA concentrates in the endosomes possibly en route toward a Golgi-endoplasmic reticulum (ER) location. Indeed, Liu et al. [19] detected anti-PSMA mAb J591 in a juxtanuclear region 2 hr after exposure to the mAb. RTA has been proposed to translocate to the cytosol of the target cell from the ER, taking advantage of the complex translocon machinery involved in the disposal of misfolded proteins [45]. If PSMA is indeed able to direct ITs to the ER, this might explain our observation that anti-PSMA RTA-based ITs, although devoid of translocation-competent domains, are endowed with great cytotoxic potential, being able to rapidly inactivate protein synthesis with a short lag phase. Efficient shuttling of ITs molecules to the ER by PSMA might also explain why addition of the RTA-ITs potentiator monensin [46,47] to the cell cultures does not further increase considerably the cytotoxic effect of anti-PSMA ITs (G. Fracasso et al., personal observation).

Effects of Anti-PSMA ITs in MTS and Clinical Setting

The best clinical setting for IT application is likely to be represented by a situation in which the tumor cell burden is low, i.e., after tumor de-bulking, in the occurrence of a minimal residual disease, or in the presence of prevascularized micrometastases. In the latter case, ITs do not need to cross the capillary basal lamina or to travel long distances within the tissues. Prostate cancer relapse after surgery is a common event, most frequently resulting from the outgrowth of minimal residual disease in the form of metastases [48]. In the metastatic disease, bone involvement is observed in most cases [48]. Prostate cancer cells disseminate to the bone marrow as small cell clusters, easily accessible through blood. Application of anti-PSMA ITs could be envisaged to eradicate small local metastases or bone marrow localization of cancer cells. To evaluate the potential of anti-PSMA ITs against 3-D tumor structures mimicking the behavior of micrometastases [20,28,43,47], we have investigated LNCaP MTS initially comprising approximately 1,000 cells. Spheroids of this size approximate the micrometastatic disease condition and can serve as a therapeutic test for investigating the cytoreductive potential of anti-PSMA ITs directed against multicellular targets. The anti-PSMA ITs must be efficacious against MTS if they are to be expected to be clinically effective against metastatic prostate carcinoma. Our results point to the effectiveness of IT therapy in small spheroids. A dose of 31.7 ng/ml J591-RTA was sufficient to sterilize all the treated MTS. Lower doses resulted in growth delay, corresponding to the elimination of various numbers of target cells of the MTS. Possible explanations of this efficient cell killing effect might be due to the following: (1) longer treatment times may allow penetration of the ITs beyond the first cell layers of the micromass, probably also bypassing possible Ag-site barrier effects [21,49–51]. (2) Internalized ITs might be recycled outside the cell and be made available for another round of binding and internalization by target cells in the vicinity [52]. Indeed, McDevitt et al. [18] reported that LNCaP cells keep binding and internalizing radiolabeled J591 mAb, probably by expression of new or recycled Ag-binding sites. Liu et al. [19] demonstrated that PSMA itself is constitutively internalized through clathrin-coated pits independently of bound mAbs and can be recycled back to the cell surface. mAb and mAb-based heteroconjugates can diffuse through tissues, despite tight junctions between cells and particularly in small 3-D structures where interstitial pressure does not represent a barrier, can reach beyond the first cell layers, travel in the intercellular space and bind target cells in the interior of the micromass [reviewed in Ref. 53]. In case of inhomogeneous expression of the cell surface target antigen, although no bystander effect in a strict sense can be envisaged when using Immunotoxins, apoptotic and necrotic processes triggered by killing Ag^+ cells would inevitably affect viability of surrounding Ag^- cells. It should also be considered that, in elaborating toxin targeting strategies, it is advisable to contemplate more than one target Ag to minimize tumor cell escape. To this end, combining Immunotoxins directed to the tumor cell and to the tumor vasculature might result in much greater anti-tumor effects. In our case, the MTS might act as a reservoir of ITs, which then reside within the MTS for long times and continue to exert their cytocidal effects against target cells. To this regard, it is also worth noticing that treatment of MTS with anti-PSMA ITs does not result in the selection of resistant cell populations, as demonstrated by our experiments where cells surviving a first cycle of treatment with ITs are again sensitive to anti-PSMA ITs after re-growth in vitro. For these reasons, the potential of anti-PSMA ITs against 3-D

structures in vivo might be even greater than that predicted based on in vitro experiments. If we extrapolate our in vitro results to a clinical situation, the dose necessary to achieve complete eradication of 125- to 150-μm-diameter cell clusters corresponds to an i.v. administration of 120.46 μg J591-smpt-nRTA, assuming the IT diffusion is initially limited to a total vascular and extracellular fluid volume of 3.8 L [54]. This amount represents only a minimal fraction of the total dose/patient administered during successful ricin- and RTA-based clinical trials [55]. Local delivery of anti-PSMA ITs might require even lower dosages. Therefore, it is likely that at these low IT dosages, side effects be considerably minimized.

Inoculation of RTA-based ITs in vivo elicits a host immune response directed against the heterologous toxin/IT introduced [3]. In some cases, the anti-RTA antibodies generated neutralized the cytotoxic potential of the injected ITs, and in most cases reported, they decreased the half-life of the ITs in the blood [3]. In most cases described, however, the tumor burden was large and schedules based on repeated injections were carried out. It is to be expected that, in the case of a micrometastatic or minimal residual disease treated with highly effective Immunotoxins and short treatment courses, the generation and adverse effects of anti-IT antibodies would be minimized. Moreover, vehicle molecules can be humanized and toxin immunogenicity can be reduced (e.g., by linkage to polyethylene glycol [56]); likely this would further diminish the risk of IT-blocking immune responses in future trials.

In Vivo Delivery

ITs can be administered systemically or locally. In the case of systemic delivery by means of blood circulation, free PSMA present in the plasma of patients could prevent binding of the IT to cell surface sites. However, this event is unlikely to take place appreciably for the following reasons: (1) unlike other prostate-related antigens, such as prostate-specific antigen, prostatic acid phosphatase, and prostate secretory protein, PSMA is an integral membrane protein, therefore, only minimal amounts are present in the circulation, mostly detectable only by very sensitive assays (i.e., Western blotting, sandwich radioimmunoassay or ELISA); (2) in patients eligible for treatment with anti-PSMA ITs serum levels of free PSMA should be low due to surgical de-bulking [57]. Moreover, (3) binding of mAb or ITs to cell surface sites is privileged with respect to binding to soluble Ag due to more favorable association kinetics [58]. In fact, presence of free soluble PSMA does not prevent acquisition of immunoscintigraphy images for diagnostic purposes when radiolabeled anti-PSMA mAb are used [17]. Therefore, it is likely that, despite the lower IT concentrations required to achieve a biological response in vivo, binding of anti-PSMA IT would not be hindered. (4) In addition, our data demonstrate that the presence of serum from patients affected by carcinoma of the prostate does not result in any significant inhibition of anti-PSMA ITs effects in vitro. Thus, it can be inferred that there are no IT blocking factors in the sera of prostate carcinoma patients and/or no breakdown of the IT molecule occurred. In any case, if release of RTA would occur in vivo, only minimal toxicity is to be expected, because RTA is far less toxic than the IT and low IT dosages would be required in the clinical setting we suggest as the most appropriate for anti-PSMA IT application in prostate cancer.

CONCLUSIONS

In conclusion, we believe that the clinical situation in prostate cancer may favor the use of anti-PSMA ITs based on a low tumor cell burden, an efficient PSMA-mediated IT internalization, a large number of PSMA sites/cell, an appreciable therapeutic window, and a fast and efficient killing of isolated target cells and of 3-D cell aggregates. In this context, the mAb J591 appears to be an interesting candidate for further developments. However, also other mAbs show properties appropriate for making efficacious anti-PSMA ITs (e.g., PEQ226.5). With the discovery of new anti-PSMA mAbs, a wider spectrum of anti-PSMA ITs might become available soon for the immunotherapy of the prostate carcinoma. Moreover, expression of PSMA at the surface of endothelial cells of the tumor microvasculature offers the opportunity of using anti-PSMA ITs as universal cytotoxic reagents to be used for the immunotherapy of different types of tumors.

ACKNOWLEDGMENTS

Dr. N.H. Bander is gratefully acknowledged for supplying the J591 monoclonal. We thank Sabrina Righetti and Elena Chiesa for their expert technical assistance. M.C. received funding from AIRC and MURST.

REFERENCES

1. Coffey DS. Prostate cancer: an overview of an increasing dilemma. Cancer 1993;71:880–886.
2. Chiarodo A. National Cancer Institute roundtable on prostate cancer: future research directions. Cancer Res 1991;51:2498–2505.
3. Thrush GR, Lark LR, Clinchy BC, Vitetta ES. Immunotoxins: an update. Annu Rev Immunol 1996;14:49–71.
4. Kreitman RJ. Immunotoxins in cancer therapy. Curr Opin Immunol 1999;11:570–578.
5. Frankel AE, Kreitman RJ, Sausville EA. Targeted toxins. Clin Cancer Res 2000;6:326–334.

6. Horoszewicz JS, Kawinski EMGP. Monoclonal antibodies to a new antigenic marker in epithelial cells and serum of prostatic cancer patients. Anticancer Res 1987;7:927–935.
7. Heston WD. Characterization and glutamyl preferring carboxypeptidase function of prostate specific membrane antigen: a novel folate hydrolase. Urology 1997;49(Suppl 3A):104–112.
8. Zhang S, Zhang HS, Reuter VE, Slovin SF, Scher HI, Livingston PP. Expression of potential target antigens for immunotherapy on primary and metastatic prostate cancers. Clin Cancer Res 1998;4:295–302.
9. Lopes AD, Davis WL, Rosenstraus MJ, Uveges AJ, Gilman SC. Immunohistochemical and pharmacokinetic characterization of the site-specific immunoconjugate CYT-356 derived from anti-prostate monoclonal antibody 7E11-C5. Cancer Res 1990;50: 6423–6429.
10. Wright GL, Haley C, Beckett ML, Schellhammer PF. Expression of prostate-specific membrane antigen in normal, benign, and malignant prostate tissue. Urol Oncol 1995;1:18–28.
11. Troyer JK, Beckett ML, Wright GL. Detection and characterization of the prostate-specific membrane antigen (PSMA) in tissue extracts and body fluids. Int J Cancer 1995;62:552–558.
12. Israeli RS, Powell CT, Corr JG, Fair WR, Heston WD. Expression of the prostate-specific membrane antigen. Cancer Res 1994;54: 1807–1811.
13. Wright GL, Grob BM, Haley C, Grossman K, Newhall K, Petrylak D, Troyer J, Konchuba A, Schellhammer PF, Moriarty R. Up-regulation of prostate-specific membrane antigen after androgen-deprivation therapy. Urology 1996;48:326–334.
14. Silver DA, Pellicer I, Fair WR, Heston WD, Cordon-Cardo C. Prostate-specific membrane antigen expression in normal and malignant human tissues. Clin Cancer Res 1997;3:81–85.
15. Liu H, Moy P, Kim S, Xia Y, Rajasekaran A, Navarro V, Knudsen B, Bander NH. Monoclonal antibodies to the extracellular domain of prostate-specific membrane antigen also react with tumor vascular endothelium. Cancer Res 1997;57: 3629–3634.
16. Chang SS, Reuter VE, Heston WD, Bander NH, Grauer LS, Gaudin PB. Five different anti-prostate-specific membrane antigen (PSMA) antibodies confirm PSMA expression in tumor-associated neovasculature. Cancer Res 1999;59:3192–3198.
17. Petronis JD, Regan F, Lin K. Indium-111 capromab pendetide (ProstaScint) imaging to detect recurrent and metastatic prostate cancer. Clin Nucl Med 1998;23:672–677.
18. McDevitt MR, Barendswaard E, Ma D, Lai L, Curcio MJ, Sgouros G, Ballangrud AM, Yang WH, Finn RD, Pellegrini V, Geerlings MW Jr, Lee M, Brechbiel MW, Bander NH, Cordon-Cardo C, Scheirberg DA. An alpha-particle emitting antibody ([213Bi]J591) for radioimmunotherapy of prostate cancer. Cancer Res 2000;60:6095–6100.
19. Liu H, Rajasekaran AK, Moy P, Xia Y, Kim S, Navarro V, Rahmati R, Bander NH. Constitutive and antibody-induced internalization of prostate-specific membrane antigen. Cancer Res 1998;58:4055–4060.
20. Chignola R, Foroni R, Candiani C, Franceschi A, Pasti M, Stevanoni G, Anselmi C, Tridente G, Colombatti M. Cytoreductive effects of anti-transferrin receptor immunotoxin in a multicellular tumor spheroid model. Int J Cancer 1994;57:268–274.
21. Chignola R, Anselmi C, Dalla Serra M, Franceschi A, Fracasso G, Pasti M, Chiesa E, Lord JM, Triderte G, Colombatti M. Self-potentiation of ligand-toxin conjugates containing ricin A chain fused with viral structures. J Biol Chem 1995;270:23345–23351.
22. Yuhas JM, Li AP, Martinez AO, Ladman AJ. A simplified method for the production and growth of multicellular tumor spheroids. Cancer Res 1977;37:3639–3643.
23. Scatchard D. The attractions of proteins for small molecules and ions. Ann N Y Acad Sci 1949;51:660–671.
24. Neville DM Jr, Youle RJ. Monoclonal antibody-ricin or ricin A chain hybrids: kinetic analysis of cell killing for tumor therapy. Immunol Rev 1982;62:75–91.
25. Casellas P, Bourrie BJ, Gros P, Jansen FK. Kinetics of cytotoxicity induced by immunotoxins. Enhancement by lysosomotropic amines and carboxylic ionophores. J Biol Chem 1984;259: 9359–9364.
26. Norton L. A Gompertzian model of human breast cancer growth. Cancer Res 1988;48(Pt 1):7067–7071.
27. Landaw EM, Distefano JJ III. Multiexponential, multicompartmental and non-compartmental modeling. II. Data analysis and statistical considerations. Am J Physiol 1984;246:R665–R677.
28. Demicheli R, Foroni R, Giuliani FC, Savi G. Influence of tumor growth kinetics on response to doxorubicin treatment of C3H mammary carcinoma. Tumori 1988;74:269–274.
29. Grauer LS, Lawler KD, Marignac JL, Kumar A, Goel AS, Wolfert RL. Identification, purification, and subcellular localization of prostate- specific membrane antigen PSM′ protein in the LNCaP prostatic carcinoma cell line. Cancer Res 1998;58:4787–4789.
30. Dautry-Varsat A, Ciechanover A, Lodish HF. pH and the recycling of transferrin during receptor-mediated endocytosis. Proc Natl Acad Sci USA 1983;80:2258–2262.
31. Trowbridge IS, Domingo DL. Anti-transferrin receptor monoclonal antibody and toxin-antibody conjugates affect growth of human tumor cells. Nature 1981;294:171–173.
32. Pirker R, FitzGerald DJ, Hamilton TC, Ozols RF, Willingham MC, Pastan I. Anti-transferrin receptor antibody linked to Pseudomonas exotoxin as a model immunotoxin in human ovarian carcinoma cell lines. Cancer Res 1985;45:751–757.
33. Colombatti M, Bisconti M, Dell'Arciprete L, Gerosa MA, Tridente G. Sensitivity of human glioma cells to cytotoxic heteroconjugates. Int J Cancer 1988;42:441–448.
34. Ballangrud AM, Yang WH, Charlton DE, McDevitt MR, Hamacher KA, Panageas KS, Ma D, Bander NH, Schenberg DA, Sgouros G. Response of LNCaP spheroids after treatment with an alpha-particle emitter (213Bi)-labeled anti-prostate-specific membrane antigen antibody (J591). Cancer Res 2001;61: 2008–2014.
35. Thorpe PE, Wallace PM, Knowles PP, Relf MG, Brown AN, Watson GJ, Knyba RE, Wawrzynczak EJ, Blakey DC. New coupling agents for the synthesis of immunotoxins containing a hindered disulfide bond with improved stability in vivo. Cancer Res 1987;47:5924–5931.
36. Thorpe PE, Wallace PM, Knowles PP, Relf MG, Brown AN, Watson GJ, Blakey DC, Newell DR. Improved antitumor effects of immunotoxins prepared with deglycosylated ricin A-chain and hindered disulfide linkages. Cancer Res 1988;48:6396–6403.
37. Foxwell BM, Donovan TA, Thorpe PE, Wilson G. The removal of carbohydrates from ricin with endoglycosidases H, F, and D and alpha-mannosidase. Biochim Biophys Acta 1985;840:193–203.
38. Kimura Y, Hase S, Kobayashi Y, Kyogoku Y, Ikenaka T, Funatsu G. Structures of sugar chains of ricin D. J Biochem (Tokyo) 1988;103:944–949.
39. Newton DL, Wales R, Richardson PT, Walbridge S, Saxena SK, Ackerman EJ, Roberts LM, Lord JM, Youle RJ. Cell surface and intracellular functions for ricin galactose binding. J Biol Chem 1992;267:11917–11922.

40. Esworthy RS, Neville DM Jr. A comparative study of ricin and diphtheria toxin-antibody-conjugate kinetics on protein synthesis inactivation. J Biol Chem 1984;259:11496–11504.
41. Chignola R, Anselmi C, Franceschi A, Pasti M, Candiani C, Tridente G, Colombatti M. Sensitivity of human leukemia cells in exponential or stationary growth phase to anti-CD5 immunotoxins. Role of intracellular processing events. J Immunol 1994; 152:2333–2343.
42. Ballangrud AM, Yang WH, Dnistrian A, Lampen NM, Sgouros G. Growth and characterization of LNCaP prostate cancer cell spheroids. Clin Cancer Res 1999;5(Suppl 10):3171s–3176s.
43. Chignola R, Foroni R, Franceschi A, Pasti M, Candiani C, Anselmi C, Fracasso G, Tridente G, Colombatti M. Heterogeneous response of individual multicellular tumour spheroids to immunotoxins and ricin toxin. Br J Cancer 1995;72:607–614.
44. Bacich DJ, Pinto JT, Tong WP, Heston WD. Cloning, expression, genomic localization, and enzymatic activities of the mouse homolog of prostate-specific membrane antigen/NAALADase/folate hydrolase. Mamm Genome 2001;12:117–123.
45. Lord JM, Roberts LM. Toxin entry: retrograde transport through the secretory pathway. J Cell Biol 1998;140:733–736.
46. Raso V, Lawrence J. Carboxylic ionophores enhance the cytotoxic potency of ligand- and antibody-delivered ricin A chain. J Exp Med 1984;160:1234–1240.
47. Colombatti M, Dell'Arciprete L, Chignola R, Tridente G. Carrier protein-monensin conjugates: enhancement of immunotoxin cytotoxicity and potential in tumor treatment. Cancer Res 1990; 50:1385–1391.
48. Scher HI, Chung LW. Bone metastases: improving the therapeutic index. Semin Oncol 1994;21:630–656.
49. Fujimori K, Covell DG, Fletcher JE, Weinstein JN. Modeling analysis of the global and microscopic distribution of immunoglobulin G, F(ab')2, and Fab in tumors. Cancer Res 1989;49: 5656–5663.
50. Fujimori K, Covell DG, Fletcher JE, Weinstein JN. A modeling analysis of monoclonal antibody percolation through tumors: a binding-site barrier. J Nucl Med 1990;31:1191–1198.
51. Weinstein JN, Eger RR, Covell DG, Black CD, Mulshine J, Carrasquillo JA, Larson SM, Keenan AM. The pharmacology of monoclonal antibodies. Ann N Y Acad Sci 1987;507:199–210.
52. Ravel S, Colombatti M, Casellas P. Internalization and intracellular fate of anti-CD5 monoclonal antibody and anti-CD5 ricin A-chain immunotoxin in human leukemic T cells. Blood 1992;79:1511–1517.
53. Fracasso G, Colombatti M. Effect of therapeutic macromolecules in spheroids. Crit Rev Oncol Hematol 2000;36:159–178.
54. Snyder WS. The standard man in relation to internal radiation dose concepts. Am Ind Hyg Assoc J 1966;27:539–545.
55. Frankel AE, FitzGerald D, Siegall C, Press OW. Advances in immunotoxin biology and therapy: a summary of the Fourth International Symposium on Immunotoxins. Cancer Res 1996; 56:926–932.
56. Hu RG, Zhai QW, He WJ, Mei L, Liu WY. Bioactivities of ricin retained and its immunoreactivity to anti-ricin antibodies alleviated through pegylation. Int J Cell Biol 2002;34:396–402.
57. Beckett ML, Cazares LH, Vlahou A, Schellhammer PF, Wright GL. Prostate-specific membrane antigen levels in sera from healthy men and patients with benign prostate hyperplasia or prostate cancer. Clin Cancer Res 1999;5:4034–4040.
58. Mason DW, Williams AF. The kinetics of antibody binding to membrane antigens in solution and at the cell surface. Biochem J 1980;187:1–20.